Analysis of Dielectric-Loaded Cavities Using an Orthonormal-Basis Method

Juan A. Monsoriu, Miguel V. Andrés, *Member, IEEE*, Enrique Silvestre, Albert Ferrando, and Benito Gimeno, *Member, IEEE*

***Abstract*—An orthonormal-basis method to analyze dielectric-loaded cavities is proposed. Resonant frequencies and fields are obtained by solving an eigenvalue problem in which the modes of an auxiliary problem define the orthonormal-basis that is used to expand the fields of the original problem. The merit of our approach is to take advantage of some mathematical properties to develop a computationally efficient and versatile method. The accuracy of the method is demonstrated by comparing our results with other results available in the literature.**

***Index Terms*—Dielectric resonators, moment methods.**

I. Introduction

In this paper, we develop an orthonormal-basis method specifically well suited for dielectric-loaded cavities. Once Maxwell's equations are written to obtain the frequencies and fields of inhomogeneous cavities by solving an eigenvalue problem, we take the modes of an auxiliary problem as an orthonormal basis to expand the fields of the original problem. Combining such an expansion with the method of moments, we obtain a matrix representation of the differential equation whose eigenvalues and eigenfunctions are the frequencies and the fields of the cavity modes, respectively. Our approach takes advantage of some mathematical properties and leads to a computationally efficient and versatile method as a function of the appropriate choice of the auxiliary problem. Here, we focus on isotropic and nonmagnetic media, but the method could be extended to cover anisotropic and magnetic media as well.

The orthonormal-basis method developed here shows a clear formal parallelism with the bi-orthonormal-basis method previously developed to analyze inhomogeneous waveguides [1], [2].

Dielectric-loaded cavities find increasing applications as microwave filters in satellite and mobile communications because of their small size, low loss, and temperature stability. The tools that are being used to simulate such cavities are basically finite-element techniques [3], finite-difference techniques [4], [5], and moment methods [6]–[9]. Among the moment-method techniques, the main differences arise from the integral or differential equation to be solved and the basis functions that are used for the expansion of the fields. In our case, the formulation of the problem is rather compact and leads to a standard eigenvalue equation. As we will show, the peculiarities of our approach may give some advantages at specific cases and provide high numerical precision, which is a requirement to model high-Q resonators.

First, we present the theoretical formulation of our method and we discuss some considerations to implement the method and the numerical advantages that can be obtained. We then focus on different examples to compare our results with others reported in the literature.

Manuscript received July 5, 2001. This work was supported by the Ministerio de Ciencia y Tecnología under Grant TIC2000-0591-C03-01.

J. A. Monsoriu, M. V. Andrés, and B. Gimeno are with the Departamento de Física Aplicada, Institut de Ciència dels Materials, Universitat de València, E-46100 Burjassot, Spain.

E. Silvestre and A. Ferrando are with the Departamento de D'Óptica, Universitat de València, E-46100 Burjassot, Spain.

Digital Object Identifier 10.1109/TMTT.2002.804648

II. Theoretical Formulation

From Maxwell's equations, harmonic magnetic and electric fields $\mathbf{H}$ and $\mathbf{E}$ in an inhomogeneously dielectric-filled cavity satisfy the differential equations

$$\left\{\nabla\times\left[\frac{1}{\varepsilon_r(\mathbf{r})}\nabla\times\circ\right]\right\}\mathbf{H}=\frac{\omega^2}{c^2}\mathbf{H} \tag{1}$$

$$\left\{\frac{1}{\varepsilon_r(\mathbf{r})}\nabla\times[\nabla\times\circ]\right\}\mathbf{E}=\frac{\omega^2}{c^2}\mathbf{E} \tag{2}$$

where an isotropic and nonmagnetic medium is assumed, enclosed by a perfect conductor, whose relative dielectric permittivity is $\varepsilon_r(\mathbf{r})$, and where c and ω are the velocity of light and the angular frequency, respectively.

In addition to (1) and (2), the fields $\mathbf{H}$ and $\mathbf{E}$ have to satisfy the equations

$$\nabla H=0 \tag{3}$$

$$\nabla[\varepsilon_r(\mathbf{r})\mathbf{E}]=0. \tag{4}$$

Since our interest is in inhomogeneous cavities and (4) limits the formulation of straightforward field expansions, it is worthwhile to use the displacement field $\mathbf{D}$ to formulate the problem. The differential equations that D has to satisfy are

$$\left\{\nabla\times\left[\nabla\times\frac{1}{\varepsilon_r(\mathbf{r})}\circ\right]\right\}\mathbf{D}=\frac{\omega^2}{c^2}\mathbf{D} \tag{5}$$

$$\nabla\mathbf{D}=0 \tag{6}$$

For cavities bounded by perfect electric conductors and filled with a nonabsorbent medium, i.e., $\varepsilon_r(\mathbf{r})$ is a real function, we can define two inner products for the magnetic and displacement fields in the form

$$\langle\mathbf{H}_i\,|\,\mathbf{H}_j\rangle_{\mathbf{H}}=\int_V\mathbf{H}_i^*\mathbf{H}_j dV \tag{7}$$

$$\langle\mathbf{D}_i\,|\,\mathbf{D}_j\rangle_{\mathbf{D}}=c^2\int_V\frac{\mathbf{D}_i^*\mathbf{D}_j}{\varepsilon_r(\mathbf{r})}dV \tag{8}$$

where $*$ denotes the complex conjugated, Z_0 is the vacuum impedance, and V is the volume of the cavity. Although, at this moment, we consider the specific case of a nonabsorbent medium, we shall see later that our method can be used to obtain the resonances of cavities filled with absorbent media. In this paper, we consider nonmagnetic materials and, for this reason, we can chose the definition of the inner product for the magnetic field equal to the ordinary scalar product. The different definition of the inner products for the displacement and magnetic fields is not arbitrary, but particularly useful because, in this way, if we express (1) and (5) in operator form as follows:

$$L_{\mathbf{H}}\mathbf{H} = \frac{\omega^2}{c^2}\mathbf{H}$$
$$L_{\mathbf{H}} \equiv \nabla \times \left[\frac{1}{\varepsilon_r(\mathbf{r})}\nabla \times \circ\right] \tag{9}$$
$$L_{\mathbf{D}}\mathbf{D} = \frac{\omega^2}{c^2}\mathbf{D}$$
$$L_{\mathbf{D}} \equiv \nabla \times \left[\nabla \times \frac{1}{\varepsilon_r(\mathbf{r})} \circ\right] \tag{10}$$

then we find that the linear operators $L_{\mathbf{H}}$ and $L_{\mathbf{D}}$ are self-adjoint, with respect to their corresponding inner products, and that their eigenfunctions $\mathbf{H}_i$ and $\mathbf{D}_i$ define two orthonormal-basis equations as follows:

$$\langle \mathbf{H}_i \,|\, L_{\mathbf{H}}\mathbf{H}_j\rangle_{\mathbf{H}} = \langle L_{\mathbf{H}}\mathbf{H}_i \,|\, \mathbf{H}_j\rangle_{\mathbf{H}}$$
$$\langle \mathbf{H}_i \,|\, \mathbf{H}_j\rangle_{\mathbf{H}} = \delta_{ij} \tag{11}$$
$$\langle \mathbf{D}_i \,|\, L_{\mathbf{D}}\mathbf{D}_j\rangle_{\mathbf{D}} = \langle L_{\mathbf{D}}\mathbf{D}_i \,|\, \mathbf{D}_j\rangle_{\mathbf{D}}$$
$$\langle \mathbf{D}_i \,|\, \mathbf{D}_j\rangle_{\mathbf{D}} = \delta_{ij}. \tag{12}$$

In consequence, the eigenvalues $(\omega/c)^2$ will be real and the eigenfunctions can be chosen to be real without loss of generality.

The above basic equations provide the framework of the orthonormal-basis method that we have developed to obtain the frequencies and fields of inhomogeneous cavities. If we provide a matrix representation of the above operators, then the problem is reduced to a standard diagonalization process of the self-adjoint operators $L_{\mathbf{H}}$ and $L_{\mathbf{D}}$. Thus, if we want to solve a problem defined by a cavity of volume V bounded by a perfect electric conductor and filled with an inhomogeneous medium defined by $\varepsilon_r(\mathbf{r})$, all that we need to know is the solution for the same cavity when it is filled with a medium characterized by $\tilde{\varepsilon}_r(\mathbf{r})$. We will refer to this second cavity as the auxiliary system, which may correspond to an empty cavity, a homogeneous cavity, or an inhomogeneous cavity. The auxiliary system will be defined by the operators $\tilde{L}_{\mathbf{H}}$ and $\tilde{L}_{\mathbf{D}}$ and their eigenfunctions define the orthogonal-basis equations $\{\tilde{\mathbf{H}}_i\}_{i=1}^{\infty}$ and $\{\tilde{\mathbf{D}}_i\}_{i=1}^{\infty}$ as follows:

$$\tilde{L}_{\mathbf{H}} = \nabla \times \left[\frac{1}{\tilde{\varepsilon}_r(\mathbf{r})}\nabla \times \circ\right]$$
$$\tilde{L}_{\mathbf{H}}\tilde{\mathbf{H}}_i = \frac{\tilde{\omega}_i^2}{c^2}\tilde{\mathbf{H}}_i$$
$$\left\langle \tilde{\mathbf{H}}_i \,|\, \tilde{\mathbf{H}}_j\right\rangle_{\tilde{\mathbf{H}}} = \delta_{ij}$$
$$\nabla\tilde{\mathbf{H}}_i = 0 \tag{13}$$

$$\tilde{L}_{\mathbf{D}} \equiv \nabla \times \left[\nabla \times \frac{1}{\tilde{\varepsilon}_r(\mathbf{r})} \circ\right]$$
$$\tilde{L}_{\mathbf{D}}\tilde{\mathbf{D}}_i = \frac{\tilde{\omega}_i^2}{c^2}\tilde{\mathbf{D}}_i$$
$$\left\langle \tilde{\mathbf{D}}_i \,|\, \tilde{\mathbf{D}}_j\right\rangle_{\tilde{\mathbf{D}}} = \delta_{ij}$$
$$\nabla\tilde{\mathbf{D}}_i = 0 \tag{14}$$

where $(\tilde{\omega}_i/c)^2$ are the corresponding eigenvalues, i.e., the resonant frequencies of the auxiliary system. This auxiliary orthonormal-basis equation will be used to obtain a matrix representation of the problem under consideration. First, we use the auxiliary modes $\tilde{\mathbf{H}}_i$ and $\tilde{\mathbf{D}}_i$ as the basis functions to expand the fields $\mathbf{H}_i$ and $\mathbf{D}_i$ of our problem and let

$$\mathbf{H}_i = \sum_k a_{ik}^{\mathbf{H}}\,\tilde{\mathbf{H}}_k \tag{15}$$
$$\mathbf{D}_i = \sum_k a_{ik}^{\mathbf{D}}\,\tilde{\mathbf{D}}_k \tag{16}$$

where $a_{ik}^{\mathbf{H}}$ and $a_{ik}^{\mathbf{D}}$ are the coefficients of the expansion. These expansions insure that $\mathbf{H}_i$ and $\mathbf{D}_i$ satisfy the outer boundary conditions and (3) and (6). Second, we substitute (15) and (16) in (9) and (10) and, following a standard Galerkin moment method, we use the same auxiliary basis functions as testing functions and we take the inner products as defined in (7) and (8). This results in

$$\sum_k L_{\mathbf{H}jk}\,a_{ik}^{\mathbf{H}} = \frac{\omega_i^2}{c^2}a_{ij}^{\mathbf{H}}$$
$$L_{\mathbf{H}jk} = \left\langle \tilde{\mathbf{H}}_j \,|\, L_{\mathbf{H}}\tilde{\mathbf{H}}_k\right\rangle_{\tilde{\mathbf{H}}} \tag{17}$$
$$\sum_k L_{\mathbf{D}jk}\,a_{ik}^{\mathbf{D}} = \frac{\omega_i^2}{c^2}a_{ij}^{\mathbf{D}}$$
$$L_{\mathbf{D}jk} = \left\langle \tilde{\mathbf{D}}_j \,|\, L_{\mathbf{D}}\tilde{\mathbf{D}}_k\right\rangle_{\tilde{\mathbf{D}}}. \tag{18}$$

$j = 1, 2, 3\ldots$, which can be written in matrix form as follows:

$$[L_{\mathbf{H}}]\left[a^{\mathbf{H}}\right] = \frac{\omega^2}{c^2}\left[a^{\mathbf{H}}\right] \tag{19}$$
$$[L_{\mathbf{D}}]\left[a^{\mathbf{D}}\right] = \frac{\omega^2}{c^2}\left[a^{\mathbf{D}}\right]. \tag{20}$$

$L_{\mathbf{H}jk}$ and $L_{\mathbf{D}jk}$ are the elements that define the matrices $[L_{\mathbf{H}}]$ and $[L_{\mathbf{D}}]$, respectively, and where $a_{ik}^{\mathbf{H}}$ and $a_{ik}^{\mathbf{D}}$ are the elements of the column matrices $[a^{\mathbf{H}}]$ and $[a^{\mathbf{D}}]$. These matrices $[L_{\mathbf{H}}], [L_{\mathbf{D}}], [a^{\mathbf{H}}]$, and $[a^{\mathbf{D}}]$ represent the differential operators $L_{\mathbf{H}}, L_{\mathbf{D}}$ and the eigenfunctions $\mathbf{H}$ and $\mathbf{D}$, respectively. Thus, (19) and (20) are a linear matrix representation of the differential equations (1) and (5). By solving the algebraic eigenvalue problem defined by (19) and (20), we obtain the frequencies and the fields of the cavity modes. In fact, we do not need to solve both equations. As we shall see later, the best option for the type of problem we are considering here is to start by solving (19). The diagonalization of (19) provides the resonant frequencies ω_i and the magnetic fields $\mathbf{H}_i$ in terms of the expansion coefficients $a_{ik}^{\mathbf{H}}$. Using Maxwell's equations, we can

then obtain the expansion coefficients $a_{ik}^{\mathbf{D}}$ of the displacement fields $\mathbf{D}_i$

$$a_{ij}^{\mathbf{D}} = \frac{\tilde{\omega}_j}{\omega_i} a_{ij}^{\mathbf{H}} \tag{21}$$

with no need of solving (20) to obtain $\mathbf{D}_i$ and the corresponding electric fields $\mathbf{E}_i$.

III. Implementation of the Method

In order to implement the method, we need to calculate the elements $L_{\mathbf{H}jk}$ and $L_{\mathbf{D}jk}$ to proceed later to the diagonalization of the matrices. Although (17) and (18) give formal expressions for these elements, we need to develop such expressions in terms of $\varepsilon_r(\mathbf{r})$ and $\tilde{\varepsilon}_r(\mathbf{r})$ that define the problem and auxiliary system. If we consider the operators $F_{\mathbf{H}} \equiv L_{\mathbf{H}} - \tilde{L}_{\mathbf{H}}$ and $F_{\mathbf{D}} \equiv L_{\mathbf{D}} - \tilde{L}_{\mathbf{D}}$

$$F_{\mathbf{H}} \equiv \nabla \times \left[\left(\frac{1}{\varepsilon_r(\mathbf{r})} - \frac{1}{\tilde{\varepsilon}_r(\mathbf{r})} \right) \nabla \times \circ \right] \tag{22}$$

$$F_{\mathbf{D}} \equiv \nabla \times \left[\nabla \times \left(\frac{1}{\varepsilon_r(\mathbf{r})} - \frac{1}{\tilde{\varepsilon}_r(\mathbf{r})} \right) \circ \right] \tag{23}$$

we find that

$$L_{\mathbf{H}jk} = \frac{\tilde{\omega}_j^2}{c^2} \delta_{jk} + \left\langle \tilde{\mathbf{H}}_j \,|\, F_{\mathbf{H}} \tilde{\mathbf{H}}_k \right\rangle_{\tilde{\mathbf{H}}} \tag{24}$$

$$L_{\mathbf{D}jk} = \frac{\tilde{\omega}_j^2}{c^2} \delta_{jk} + \left\langle \tilde{\mathbf{D}}_j \,|\, F_{\mathbf{D}} \tilde{\mathbf{D}}_k \right\rangle_{\tilde{\mathbf{D}}} \tag{25}$$

and substituting (22) and (23) into (24) and (25), we obtain

$$L_{\mathbf{H}jk} = \frac{\tilde{\omega}_j^2}{c^2} \delta_{jk} + \tilde{\omega}_j \tilde{\omega}_k \int_V \left(\frac{1}{\varepsilon_r} - \frac{1}{\tilde{\varepsilon}_r} \right) \tilde{\mathbf{D}}_j^* \tilde{\mathbf{D}}_k \, dV \tag{26}$$

$$L_{\mathbf{D}jk} = \frac{\tilde{\omega}_j^2}{c^2} \delta_{jk} + \tilde{\omega}_j^2 \int_V \left(\frac{1}{\varepsilon_r} - \frac{1}{\tilde{\varepsilon}_r} \right) \tilde{\mathbf{D}}_j^* \tilde{\mathbf{D}}_k \, dV. \tag{27}$$

Equations (26) and (27) permit a calculation of the elements $L_{\mathbf{H}jk}$ and $L_{\mathbf{D}jk}$ in terms of the frequencies and the electric fields of the modes of the auxiliary system. The key contributions are the second terms, which can be regarded as coupling coefficients between modes of the auxiliary basis. Such a coupling exists because of the differences between the dielectric function of the problem and that of the auxiliary system, i.e., the factor $(\varepsilon_r^{-1} - \tilde{\varepsilon}_r^{-1})$. These equations show with clarity some important properties. On the one hand, $[L_{\mathbf{H}}]$ is a Hermitian matrix since $L_{\mathbf{H}jk} = (L_{\mathbf{H}kj})^*$. In addition, the eigenfunctions of the auxiliary system can be chosen to be real to insure that all the products $\tilde{\mathbf{D}}_j^* \tilde{\mathbf{D}}_k$ are real as well. Thus, the $[L_{\mathbf{H}}]$ matrix will be real and symmetric. On the other hand, $[L_{\mathbf{D}}]$ is not a Hermitian matrix. For this reason, if we want to implement the method efficiently, the best option is to start solving the problem for the magnetic field. This option permits to take advantage of the properties of the $[L_{\mathbf{H}}]$ matrix. Later, we can compute the displacement and electric fields using (21).

The way in which we implement the method leads to a standard algebraic linear eigenvalue problem where the matrix representation of the operator is real and symmetric. This is a clear advantage with respect other modal methods in which a generalized eigenvalue equation has to be solved with non-Hermitian matrices [6]. The computing time difference between solving a standard eigenvalue problem and solving a generalized eigenvalue problem is around 15% less. If we consider the amount of available memory in the computer, e.g., 1.6 GB, the use of a real and symmetric matrix permits to diagonalize a matrix of the order of $20\,723 \times 20\,723$, while if the matrix is real, but nonsymmetric, the maximum order would be $14\,654 \times 14\,654$ and, in addition, the diagonalization of the first matrix takes less than 50% time than what is required by the second matrix. Therefore, the implementation of the orthonormal-basis method that we present in this paper combines the possibility of using a larger number of basic functions with less computing time requirements than other similar modal methods.

The choice of the auxiliary basis is an important point for an efficient implementation of the method. On the one hand, one has to consider the number of basis functions that may be required to achieve a given accuracy of the solution and the size of the matrix that can be diagonalized. On the other hand, one has to consider as well the interest of an easy and accurate evaluation of the matrix elements. If the memory available in the computer is of the order of 1 GB, it appears worthwhile to focus on an easy and analytical evaluation of the matrix elements, and then the accuracy will be determined by the number of basis functions used to expand the fields.

Although we have considered up to now the case of cavities filled with nonabsorbent materials, it is possible to obtain, as well, the resonances of lossy cavities using the modal method developed here. The key point is to realize that all what is needed to obtain a matrix representation of the operator of a given problem is the right choice of the auxiliary system. If the modes of the auxiliary system defines an orthonormal basis, then the expansion of the fields in terms of the auxiliary modes and the application of the Garlekin moment method permit to obtain a matrix representation of the operator, even for the case of a lossy cavity. Now, none of the differential operators $L_{\mathbf{H}}$ and $L_{\mathbf{D}}$ will be Hermitian and some of the previously referred numerical properties, which appeared as specific advantages of our approach, will not apply. However, the problem to be solved is still a standard linear eigenvalue system. In any case, we can always carry out most of the simulation and the design work by neglecting the cavity losses. The losses can be taken into account in the final part of the calculation, either following the above approach or a perturbative method [10].

IV. Numerical Results and Discussion

A. Cylindrical Cavity Loaded With a Dielectric Rod

The first case that we want to consider in order to test the method and to discuss its implementation is a cylindrical cavity loaded with a dielectric rod that extends along the cavity length [see Fig. 1(a)]. This is an inhomogeneous cavity with an analytical solution, thus providing us with the possibility of an accurate evaluation of the precision of the method.

We have chosen the modes of an empty cylindrical cavity as the auxiliary basis to implement the method. These auxiliary modes are denoted typically as $\mathrm{TE}_{\mathrm{nmp}}$ and $\mathrm{TM}_{\mathrm{nmp}}$ [11].

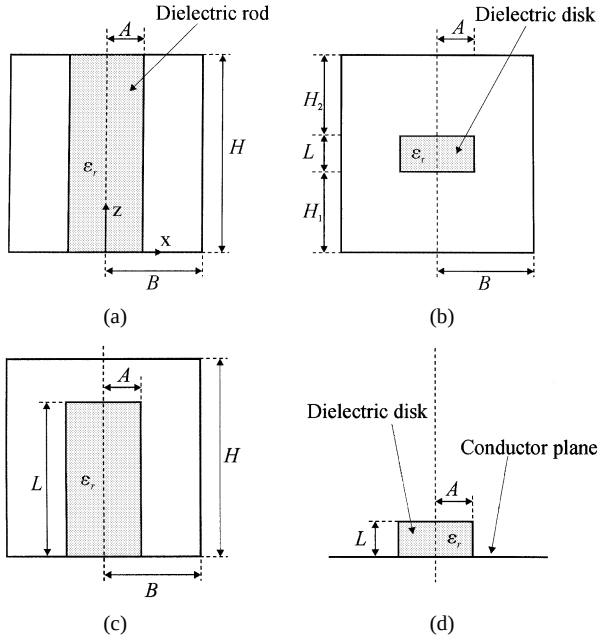

Fig. 1. Configuration of different dielectric resonators. (a) Cylindrical cavity loaded with a dielectric rod. (b) Cylindrical cavity loaded with a dielectric disk. (c) Dielectric combline resonator with a cylindrical enclosure. (d) Dielectric disk resonator on a conductor plane.

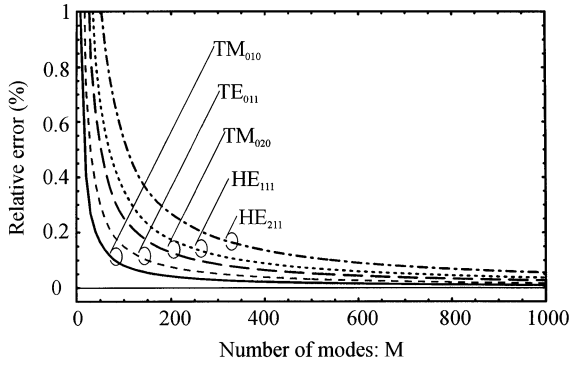

Fig. 2. Relative error of the resonant frequencies of a cylindrical cavity loaded with a dielectric rod as a function of the number of modes of the auxiliary system.

We consider each azimutal and longitudinal orders n and p separately since the coupling between modes of different azimutal and longitudinal orders is zero. In addition, we take the dependence of the modes on the azimutal angle in the form $\exp(\pm jn\phi)$. Although this choice makes the auxiliary modes to be complex, the $L_{\mathbf{H}}$ operator will remain real and symmetric because of the specific form of (26).

The choice of this auxiliary system permits an analytical evaluation of the elements of the matrix that represents the $L_{\mathbf{H}}$ operator. Thus, the precision of the method will be determined by the number of auxiliary modes used for the expansion of the fields. Fig. 2 shows the convergence of the solution as a function of the number of auxiliary modes at a constant azimutal order n for five modes of different azimutal and radial symmetries.

We can see in Fig. 2 that a relative error smaller than 1% is achieved with less than 100 auxiliary modes, which is a practically instantaneous calculation in a Cray-Silicon Graphics Origin-2000 machine. Even with such a small number of auxiliary modes, our results are better than others reported in the literature obtained with a finite-difference time-domain method [12], [13] or with a finite-element method [14]. However, by increasing the number of auxiliary modes, the errors decrease further, beyond 0.1% when 1000 auxiliary modes are used. In this case, the calculations take several seconds. Table I compares the nine lower resonant frequencies obtained with our orthonormal-basis method with the analytical solution obtained with a standard boundary value method. We can see that the difference is always smaller than 0.02% when 5000 auxiliary modes are used to expand the fields. Now it takes 15 min to solve each azimutal order. We include in Table I the values reported in [12] and [13].

TABLE I
COMPARISON OF THE LOWER ORDER RESONANT FREQUENCIES (IN GIGAHERTZ) FOR THE CYLINDRICAL CAVITY LOADED WITH A DIELECTRIC ROD ($\varepsilon_r = 37.6, A = 1.00076$ cm, $B = 1.27$ cm, $H = 1.397$ cm)

Mode	Analytical solution	Present Technique		Other method [12]
		Absolute value	Relative error (%)	
TM_{010}	1.49732	1.49738	0.004	1.47
TM_{110}	2.43331	2.43344	0.005	2.38
HE_{111}	2.50206	2.50228	0.009	2.48
TE_{011}	3.02686	3.02701	0.005	—
TM_{210}	3.32795	3.32818	0.007	—
TM_{011}	3.38932	3.38960	0.008	3.38
HE_{211}	3.42508	3.42552	0.013	3.38
TM_{020}	3.59190	3.59215	0.007	—
HE_{121}	3.81776	3.81820	0.012	3.79

Since the method provides the modal fields in addition to the frequencies of resonance, we have included in Fig. 3 some of them as an example. In this case, we show the magnetic and electric fields of the HE_{111} resonant mode. This is a hybrid mode whose fields are a combination of TE and TM modes of the auxiliary basis of azimutal and longitudinal orders $n = 1$ and $p = 1$, respectively. Fig. 3 includes two plots to illustrate the right behavior of the fields around the boundaries. In Fig. 3(e), we can see a case in which the x-component of the electric field is normal to the dielectric surface and it exhibits a discontinuity. In Fig. 3(f), we can see a case in which it is parallel to the boundary and the field is continuous, although a Gibbs effect shows up.

B. Cylindrical Cavity Loaded With a Dielectric Disk

The second structure that we analyze is shown in Fig. 1(b) and consists of a cylindrical cavity symmetrically loaded with a dielectric disk. In this case, we use the same auxiliary basis than in the previous case, i.e., the modes of the empty cavity. This option again leads to analytical expressions for the elements of the matrix $L_{\mathbf{H}}$.

This inhomogeneous cavity has been extensively used to test and compare different methods of analysis. We can compare our results with others obtained with a mode-matching method [15], a finite-element method [14], a finite-difference time-domain method [12], [13], and a frequency-domain finite-difference method [16]. Table II presents a list of all these results. In

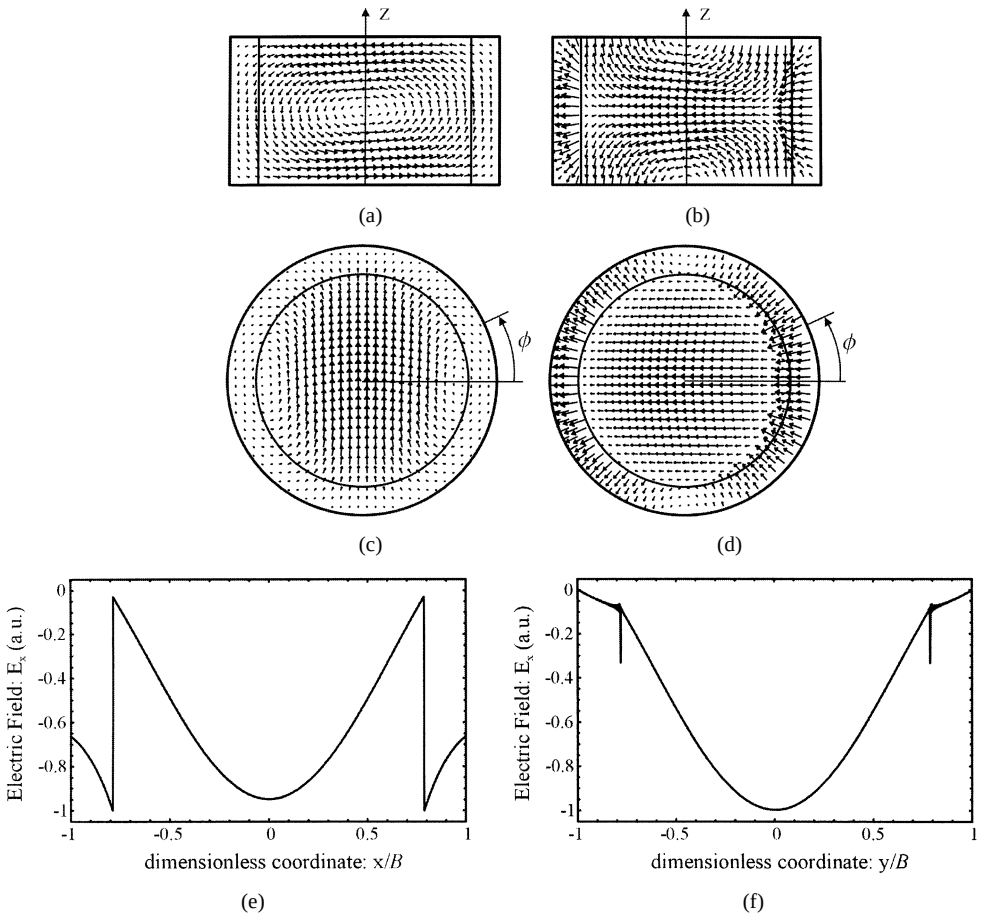

Fig. 3. Field distribution of the HE_{111} mode of a cylindrical cavity loaded with a dielectric rod. (a) Magnetic field at $\phi = \pi/2$. (b) Electric field at $\phi = 0$. (c) Magnetic field at $z = 0$. (d) Electric field at $z = H/2$. (e) x-component of the electric field along the x-axis at $z = H/2$. (f) x-component of the electric field along the y-axis at $z = H/2$.

the fourth column, we include the relative difference between our results and the results provided in [16]. In [16], an iterative method is used to solve the system of equations and the convergence with the number of iterations is insured, although there are other approximations in the method, such as the size of the grid, that may be responsible for the differences that we find in Table II with respect to our method. In the case of our method, all the figures of the numerical results shown in Table II should be virtually correct since the integral have been computed analytically and the convergence with the number of auxiliary modes has been insured. Our results have been computed with 10 000 auxiliary modes, which takes 140 min per azimutal order.

At this point, it is worthwhile to discuss some characteristics of the orthonormal-basis method that we present here. We find that the method works with the same efficiency both when the fields of the resonances have TE or TM structures and when they are hybrid modes, and that there is no specific difficulty to deal with geometrical singularities at dielectric corners and, therefore, there is no need to smooth the corners to model a dielectric resonator. In addition, our method is free of spurious modes.

C. Dielectric Combline Resonator

The third example that we consider is a dielectric combline resonator defined by a dielectric rod, mounted in a longer cylindrical enclosure $H > L$, as shown in Fig. 1(c). In this case, we have chosen the same auxiliary modes as in previous examples.

We find a good agreement between our results and those obtained with a rigorous mode-matching method [17]. Following the notation of [17], Fig. 4 gives the frequencies of resonance of the TM_{01}, TM_{02}, TE_{01}, HE_{11}, and HE_{12} modes as a function of the radius of the dielectric rod, which is in good agreement with [17].

The evaluation of losses in dielectric loaded resonators is an important point because, in general, dielectric loaded resonators have very low loss. It is precisely this property that is the most appealing feature of dielectric combline resonators when compared to conventional combline resonators. As was mentioned in Section III, the orthonormal-basis method that we present here can be applied to cavities loaded with lossy dielectrics, i.e., dielectrics with a loss tangent $\tan\delta$ different from zero. In order to illustrate this feature, we have computed the complex eigenvalues of the non-Hermitian operator $L_{\mathbf{H}}$ corresponding to a dielectric combline resonator with a lossy dielectric rod ($\varepsilon_r = 36.0, \tan\delta = 4.0 \times 10^{-5}, H = 32.00$ mm, $B = 19.05$ mm, $L = 30.48$ mm, $A = 7.112$ mm). A complex eigenvalue gives rise to a complex frequency of resonance $\omega = \omega' + j\omega''$, whose imaginary part determines the Q factor $Q = \omega'/(2\omega'')$. In this example, we compute $Q = 45\,460$ for the fundamental resonance ($\omega' = 1.879$ GHz). Since the cavity is a low-loss system,

TABLE II
COMPARISON OF THE LOWER ORDER RESONANT FREQUENCIES (IN GIGAHERTZ) FOR THE CYLINDRICAL CAVITY LOADED WITH A DIELECTRIC DISK ($\varepsilon_r = 35.74, A = 0.8636$ cm, $B = 1.295$ cm, $L = 0.762$ cm, $H_1 = H_2 = 0.381$ cm)

Mode	[15]	Present Technique		Other methods		
		Absolute value	Relative difference (%)	[13]	[12]	[14]
TE_{01}	3.429	3.444	0.44	3.435	3.53	3.428
TE_{02}	5.412	5.458	0.85	5.493	—	5.462
TE_{03}	5.908	5.944	0.61	—	—	5.93
TE_{04}	7.497	7.568	0.94	—	—	—
TE_{05}	8.015	8.100	1.05	—	—	—
TE_{06}	8.581	8.649	0.79	—	—	—
TM_{01}	4.542	4.568	0.57	4.601	4.53	4.551
TM_{02}	6.361	6.384	0.36	—	—	—
TM_{03}	7.254	7.323	0.95	—	—	7.26
TM_{04}	7.641	7.685	0.57	—	—	—
TM_{05}	9.093	9.169	0.83	—	—	—
TM_{06}	9.942	10.031	0.89	—	—	—
HE_{11}	4.205	4.251	1.09	4.271	3.90	4.224
HE_{12}	4.310	4.358	1.11	4.373	4.17	4.326
HE_{13}	5.662	5.753	1.59	—	—	5.74
HE_{14}	5.924	5.986	1.04	—	—	5.94
HE_{15}	6.331	6.397	1.04	—	—	6.36
HE_{16}	7.213	7.269	0.77	—	—	—
HE_{21}	4.992	5.041	0.98	—	—	5.00
HE_{22}	5.311	5.353	0.78	—	—	5.33
HE_{23}	6.943	7.015	1.03	—	—	—
HE_{24}	7.285	7.402	1.59	—	—	—
HE_{25}	7.355	7.423	0.92	—	—	—
HE_{26}	8.208	8.280	0.87	—	—	—
HE_{31}	5.843	5.896	0.90	—	—	5.85
HE_{32}	6.386	6.432	0.72	—	—	6.40
HE_{33}	7.901	7.981	1.01	—	—	—
HE_{34}	8.098	8.212	1.40	—	—	—
HE_{35}	8.453	8.525	0.85	—	—	—
HE_{36}	9.365	9.440	0.80	—	—	—

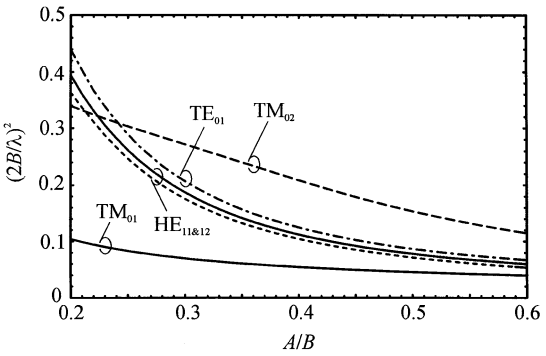

Fig. 4. Normalized resonant frequencies of a dielectric combline resonator as a function of the normalized radius of the dielectric rod.

we can validate this result with a standard perturbative calculation, using the fields of the ideal cavity to compute the losses in the dielectric. Thus, we obtain $Q = 45\,440$, which is in good agreement with our previous calculation.

D. Dielectric Disk Resonator on a Conductor Plane

The resonant frequencies of a dielectric disk placed on a conductor plate [see Fig. 1(d)] can be found with the present method by adding a metallic enclosure to define a finite cavity. In some cases, such an enclosure has no real existence and we will be interested in being able to insure that it has no significant effect on the true disk resonances. In other cases, the enclosure can be a physical shield by being part of the system. However,

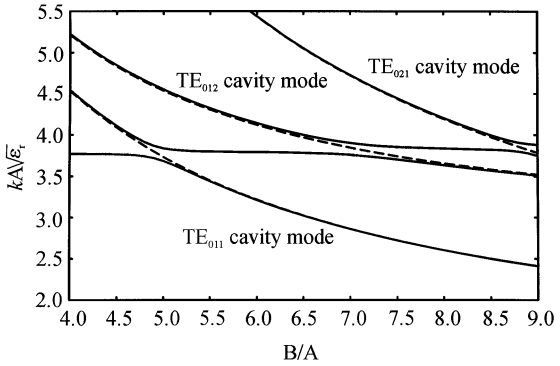

Fig. 5. Normalized resonant wavenumbers of a shielded dielectric disk as a function of the normalized radius of the enclosure.

the enclosure introduces always its cavity modes as additional resonances, which may exhibit a strong coupling with the resonances of the dielectric disk when they are close. In consequence, in both situations, one needs to control the effects of such a coupling either to know which geometries may modify substantially the properties of the disk as a resonator or to know when we may wrongly compute the resonances of the ideal unshielded disk. The dependence of the resonant modes on the size of the enclosure is specifically important in this case.

In order to formulate the method, a shielded dielectric disk can be regarded as a dielectric combline resonator described in Fig. 1(c). Now H and B will be larger than L and A. Fig. 5 presents the normalized wavenumber of the resonances of the system as a function of the normalized radius of the enclosure. The present method gives the resonances of the disk and cavity, and shows the strong coupling that some of them exhibit. We can identify in Fig. 5 the resonances of the disk as those that are virtually independent of the enclosure radius. Fig. 5 includes the resonances of an empty enclosure (dashed lines) for an easy identification of the empty cavity modes. Our results show a good agreement with those obtained with a boundary-element method [18].

E. Rectangular Cavity Loaded With a Dielectric Disk

The last example that we want to include is the case of a rectangular cavity loaded with a dielectric disk (see Fig. 6). This case is closely related to the cylindrical cavity loaded with a dielectric disk that has been previously discussed. The use of a rectangular enclosure instead of a coaxial cylinder makes an accurate simulation rather more difficult. However, the rectangular enclosure has a specific interest when coupling several cavities to design high-order filters because of the modeling of the coupling slots and good mechanical stability.

To model this case, we have chosen the modes of an empty rectangular cavity as the auxiliary basis, i.e., the well-known $\mathrm{TE}_{\mathrm{nmp}}$ and $\mathrm{TM}_{\mathrm{nmp}}$ modes [19]. As before, this choice permits an analytical evaluation of the elements of the matrix $L_{\mathbf{H}}$.

Using the present technique, no staircasing procedure is required to simulate curved dielectric surfaces. The implementation of the method for this case has an important difference with respect to previous cases. Now, the modes of the problem and the auxiliary modes do not share a given symmetry and, as a consequence, the diagonalization of the matrix cannot be reduced

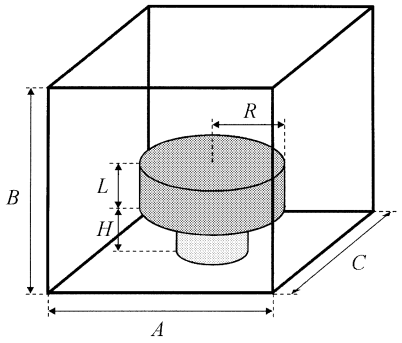

Fig. 6. Configuration of a dielectric disk resonator in a rectangular cavity.

TABLE III
COMPARISON OF THE RESONANT FREQUENCY (IN GIGAHERTZ) OF THE $\mathrm{HEM}_{11\delta}$ MODE FOR DIFFERENT DIELECTRIC DISKS IN A RECTANGULAR ENCLOSURE ($A = B - 2.54$ cm, $C = 2.377$ cm, $H = 0.699$ cm, $\varepsilon_r = 38$)

Disk size		Theroretical simulations				Experimental
R (cm)	L (cm)	Present Technique	[5]	[19]	[20]	[20]
0.831	0.554	4.391	4.388	4.40	4.388	4.382
0.875	0.584	4.168	4.163	4.17	4.161	4.153
0.961	0.643	3.762	3.725	3.78	3.721	3.777

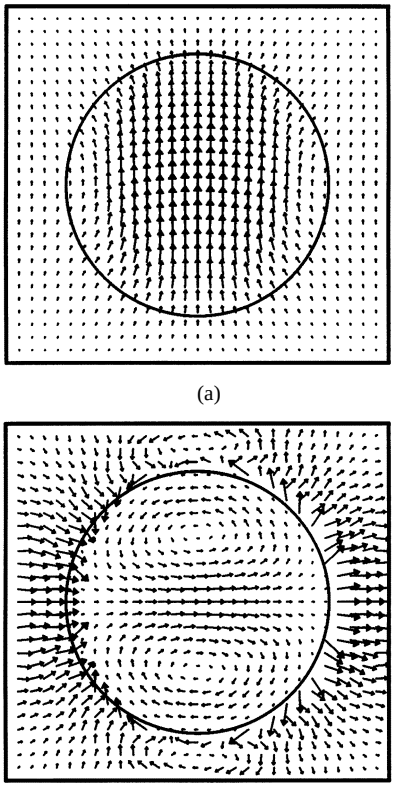

(a)

(b)

Fig. 7. Modal field distribution for the $\mathrm{HEM}_{11\delta}$ mode of a dielectric disk resonator in a rectangular cavity, at the central cross section of the disk with $A = B = 2.54$ cm, $C = 2377$ cm, $H = 0.699$ cm, $\varepsilon_r = 38$ $R = 0.875$ cm, and $L = 0.584$ cm. (a) Magnetic field. (b) Electric field.

to the diagonalization of a series of submatrices, as we did in the previous cases considering each azimutal order separately. Thus, to achieve a given numerical accuracy, we need a relatively higher number of modes than in previous cases.

We have used 20 000 auxiliary modes to compute the results that we present in Table III. Table III is a comparison between our results and the data obtained with a finite-difference time-domain method [5], [20] and a mode-matching method [21], as well as with the experimental values reported in [21]. A very good agreement is shown in Table III. In our simulation, we have assumed that the support of the dielectric disk has $\varepsilon_r = 1$, as in the simulations we use for comparison. Fig. 7 gives the modal field distribution for the first $\mathrm{HE}_{11\delta}$ mode, which agrees with the results reported in [20] and [21].

V. CONCLUSION

The orthonormal-basis method that has been formulated in this paper is an efficient method to analyze inhomogeneous cavities. The method has been verified by comparing the results with theoretical and experimental data available in the literature for both cylindrical and rectangular enclosures filled with dielectric rods. Our theoretical approach has not been limited to lossless dielectrics and we have provided an example to demonstrate the capability of the method to include the dielectric losses directly in its formulation. The method is free of spurious modes and uses no staircase approximation to deal with curved surfaces of the dielectrics. In fact, in most cases, such as in the examples that have been provided in this paper, the method can be formulated analytically, insuring a high numerical accuracy; the finite number of modes used for the expansion of the fields being the only numerical approximation.

REFERENCES

[1] E. Silvestre, M. V. Andrés, and P. Andrés, "Biorthonormal-basis method for the vector description of optical-fiber modes," *J. Lightwave Technol.*, vol. 16, pp. 923–928, May 1998.
[2] E. Silvestre, M. A. Abiá, B. Gimeno, A. Ferrando, M. V. Andrés, and V. E. Boria, "Analysis of inhomogeneously filled waveguides using a bi-orthonormal-basis method," *IEEE Trans. Microwave Theory Tech.*, vol. 48, pp. 589–596, Apr. 2000.
[3] D. Baillargeat, S. Verdeyme, M. Aubourg, and P. Guillon, "CAD applying the finite-element method for dielectric-resonator filters," *IEEE Trans. Microwave Theory Tech.*, vol. 46, pp. 10–17, Jan. 1998.
[4] J. M. Guan and C. C. Su, "Resonant frequencies and field distributions for the shielded uniaxially anisotropic dielectric resonator by the FD–SIC method," *IEEE Trans. Microwave Theory Tech.*, vol. 45, pp. 1767–1777, Oct. 1997.
[5] W. Yu and R. Mittra, "Resonant frequencies and field distributions for the shielded uniaxially anisotropic dielectric resonator by the FD–SIC method," *IEEE Microwave Wireless Comp. Lett.*, vol. 11, pp. 25–27, Jan. 2001.
[6] R. F. Harrington, *Field Computation by Moment Methods.* Piscataway, NJ: IEEE Press, 1993, pp. 172–188.
[7] J. Krupta, "Resonant modes in shielded cylindrical ferrite and single-crystal dielectric resonators," *IEEE Trans. Microwave Theory Tech.*, vol. 37, pp. 691–697, Apr. 1989.
[8] S. L. Lin and G. W. Hanson, "An efficient full-wave method for analysis of dielectric resonators possessing separable geometries immersed in inhomogeneous environments," *IEEE Trans. Microwave Theory Tech.*, vol. 48, pp. 84–82, Jan. 2000.
[9] C. Wang and K. A. Zaki, "Generalized multilayer anisotropic dielectric resonators," *IEEE Trans. Microwave Theory Tech.*, vol. 48, pp. 60–66, Jan. 2000.
[10] J. D. Jackson, *Classical Electrodynamics*, 2nd ed. New York: Wiley, 1975, pp. 356–360.
[11] C. A. Balanis, *Advanced Engineering Electromagnetics.* New York: Wiley, 1989, pp. 352–394.

[12] P. H. Harms, J. F. Lee, and R. Mittra, "A study of the nonorthogonal FDTD method versus the conventional FDTD technique for computing resonant frequencies of cylindrical cavities," *IEEE Trans. Microwave Theory Tech.*, vol. 40, pp. 741–746, Apr. 1992.
[13] ——, "Corrections to 'A study of the nonorthogonal FDTD method versus the conventional FDTD technique for computing resonant frequencies of cylindrical cavities'," *IEEE Trans. Microwave Theory Tech.*, vol. 40, pp. 2215–2216, Apr. 1992.
[14] M. M. Thaheri and D. Mirshekar-Syahkal, "Accurate determination of modes in dielectric loaded cylindrical cavities using a one-dimensional finite element method," *IEEE Trans. Microwave Theory Tech.*, vol. 37, pp. 1536–1540, Oct. 1989.
[15] K. A. Zaki and C. Chen, "New results in dielectric-loaded resonator," *IEEE Trans. Microwave Theory Tech.*, vol. MTT-34, pp. 815–824, Jan. 1986.
[16] C. C. Su and J. M. Guan, "Finite-difference analysis of dielectric-loaded cavities using the simultaneous iteration of the power method with the Chebyshev acceleration technique," *IEEE Trans. Microwave Theory Tech.*, vol. 42, pp. 1998–2006, Oct. 1994.
[17] C. Wang, K. A. Zaki, A. E. Atia, and T. G. Dolan, "Dielectric combline resonators and filters," *IEEE Trans. Microwave Theory Tech.*, vol. 46, pp. 2501–2506, Dec. 1998.
[18] R. E. Collin and D. A. Ksienski, "Boundary element method for dielectric resonators and waveguides," *Radio Sci.*, vol. 22, pp. 1155–1167, Dec. 1987.
[19] C. A. Balanis, *Advanced Engineering Electromagnetics*. New York: Wiley, 1989, pp. 470–499.
[20] N. Kaneda, B. Houshmand, and T. Itoh, "FDTD analysis of dielectric resonators with curved surfaces," *IEEE Trans. Microwave Theory Tech.*, vol. 45, pp. 1645–1649, Sept. 1997.
[21] X. P. Liang and K. A. Zaki, "Modeling of cylindrical dielectric resonators in rectangular waveguides and cavities," *IEEE Trans. Microwave Theory Tech.*, vol. 41, pp. 2174–2181, Dec. 1993.

Juan A. Monsoriu was born in València, Spain, in 1975. He received the Licenciado degree in physics and Master's degree in optics from the Universidad de València (UV), Burjassot, Spain, in 1998 and 2000, respectively, and is currently working toward the Ph.D. degree in physics at UV.

Since 2000, he has been an Assistant Professor with the Departamento de Física Aplicada, Universidad Politécnica de València. His research interests are modal methods for the design of inhomogeneous waveguides and dielectric resonators.

Miguel V. Andrés (M'91) was born in València, Spain, in 1957. He received the Licenciado en Física degree and Doctor en Física (Ph.D.) degree from the Universidad de València, Burjassot, Spain, in 1979 and 1985, respectively.

Since 1983, he has served successively as an Assistant Professor and Lecturer in the Departamento de Física Aplicada, Universidad de València. From 1984 to 1987, he was with the Department of Physics, University of Surrey, U.K., as a Visiting Research Fellow. Until 1984, he was engaged in research on microwave surface waveguides. His current research interests include optical fiber components based on tapers, Bragg gratings and photonic crystal fibers and their applications for signal processing, microwave photonics and sensors, and waveguide theory.

Dr. Andrés is a member of the Optical Society of America (OSA) and the Institute of Physics (IOP).

Enrique Silvestre was born in València, Spain, in 1962. He received the Licenciado degree in physics, M.Sc. degree in theoretical physics, M.Sc. degree in optics, and Ph.D. degree in optics from the Universitat de València (UV), Burjassot, Spain, in 1986, 1989, 1997, and 1999, respectively.

In 1997, he was an Assistant Professor with the Departamento de D'Óptica, UV. From 1999 to 2000, he was with the Department of Physics, University of Bath, Bath, U.K., where he was a Research Officer. Since 2001, he has been an Associate Professor with UV. His research interests are modal techniques for electromagnetic-wave propagation in nonsymmetrical structures and photonic crystals.

Albert Ferrando was born in València, Spain, in 1963. He received the Licenciado en Física and M.Sc. and Ph.D. degrees in theoretical physics from the Universitat de València (UV), Burjassot, Spain, in 1985, 1986 and 1991, respectively.

His professional affiliations have included UV, the Universidad Autónoma de Madrid (1990–1991), Madrid, Spain, where he was an Assistant Professor, and the Universisty of Bern (1991–1993), Bern, Switzerland, where he was a Post-Doctoral Fellow. He was also a Visiting Scientist with the Niels Borh Institute (1988), Copenhagen, Denmark, and the Massachusetts Institute of Technology (1995, 1996, 1998, 1999, and 2001), Cambridge. In 1996, he joined the Departamento de D'Óptica, UV, as an Assistant Professor and became an Associate Professor in 2001. His research interests are electromagnetic propagation in optical waveguides and fiber devices, as well as nonlinear and quantum effects in optical fibers.

Benito Gimeno (M'01) was born in València, Spain, on January 29, 1964. He received the Licenciado degree in physics and Ph.D. degree from the Universidad de València, Burjassot, Spain, in 1987 and 1992, respectively.

From 1987 to 1990, he was a Fellow with the Universidad de València. Since 1990, he has been an Assistant Professor with the Departmento de Física Aplicada, Universidad de València, where he became Associate Professor in 1997. From 1994 to 1995, he was a Research Fellow with the European Space Research and Technology Centre of the European Space Agency (ESTEC). His current research interests include the areas of computer-aided techniques for analysis of microwave passive components, waveguide structures including dielectric resonators, and photonic crystals.